Lin *et al. Cell Communication and Signaling* (2025) 23:132
https://doi.org/10.1186/s12964-025-02126-x

Cell Communication and Signaling

RESEARCH Open Access

Upregulated FSP1 by GPD1/1L mediated lipid droplet accumulation enhances ferroptosis resistance and peritoneal metastasis in gastric cancer

Guoliang Lin[1,2†], Qingnan Liu[1,2†], Chengjie Xie[2], Ke Ding[2], Guanghua Mo[2], Lu Zeng[2], Fan Zhang[2], RuiXuan Liu[1], Lei Lu[2], Wei Hong[2], Yuling Mao[3], Haibo Su[1,2*] and Shuai Li[1,2*]

Abstract

To successfully metastasize, cancer cells must evade detachment induced cell death, known as anoikis. Unraveling the mechanisms that gastric cancer (GC) circumvent anoikis and achieve peritoneal metastasis especially during unanchored growth, could significantly improve patient outcomes. Our study reveals that GC cells exhibit increased lipid peroxidation, MDA production, and cell death during suspension culture, which can be mitigated by the intervention with liproxstatin-1 and ferrostatin-1. We discovered that oleic acid (OA) or adipocytes stimulate lipid accumulation in GC cells, thereby inhibiting lipid peroxidation and cell death. Lipid mass spectrometry confirmed an upregulation of triglyceride synthesis, indicating that the accumulation of lipid droplet may confer resistance to ferroptosis during suspension growth. In vitro assays demonstrated that OA not only induces lipid droplet accumulation but also upregulates the expression of ferroptosis suppressor protein 1 (FSP1), a process that can be abrogated by the double knockout of GPD1/1L genes. Additionally, we have demonstrated that a decrease in the ubiquitination of FSP1 in GC cells upon lipid droplet accumulation, as well as silencing or pharmacological targeting FSP1, promotes ferroptosis and disrupts the peritoneal metastatic potential of GC cells. Collectively, our findings highlight the potential of FSP1 as a promising therapeutic target for metastatic gastric cancer.

Keywords FSP1, Lipid droplet, Gastric cancer, Ferroptosis

†Guoliang Lin and Qingnan Liu contributed equally to this work.

*Correspondence:
Haibo Su
suhaibo899@163.com
Shuai Li
gundam-speed@163.com
[1]Guangzhou Institute of Cancer Research, The Affiliated Cancer Hospital, Guangzhou Medical University, Guangzhou 511436, PR China
[2]GMU-GIBH Joint School of Life Sciences, The Guangdong-Hong Kong-Macao Joint Laboratory for Cell Fate Regulation and Diseases, Guangzhou Medical University, Guangzhou 511436, PR China
[3]Key Laboratory for Reproductive Medicine of Guangdong Province, The Third Affiliated Hospital of Guangzhou Medical University, Guangzhou 511436, PR China

© The Author(s) 2025. **Open Access** This article is licensed under a Creative Commons Attribution-NonCommercial-NoDerivatives 4.0 International License, which permits any non-commercial use, sharing, distribution and reproduction in any medium or format, as long as you give appropriate credit to the original author(s) and the source, provide a link to the Creative Commons licence, and indicate if you modified the licensed material. You do not have permission under this licence to share adapted material derived from this article or parts of it. The images or other third party material in this article are included in the article's Creative Commons licence, unless indicated otherwise in a credit line to the material. If material is not included in the article's Creative Commons licence and your intended use is not permitted by statutory regulation or exceeds the permitted use, you will need to obtain permission directly from the copyright holder. To view a copy of this licence, visit http://creativecommons.org/licenses/by-nc-nd/4.0/.

Introduction

GC is recognized as one of the most prevalent malignancies globally, consistently ranking within the top five in incidence and alarmingly, among the top three in mortality rates [1]. The gravity of the situation was underscored in 2020 with an estimated over 1 million new cases diagnosed worldwide, tragically culminating in nearly 769,000 fatalities [2]. While early-stage gastric cancer is typically associated with a highly favorable prognosis, with an impressive 5-year survival rate exceeding 90%, its early identification remains elusive. The challenge stems from the cancer's subtle onset, often presenting with either no symptoms or vague indicators such as mild indigestion. The situation is further exacerbated by a general lack of public knowledge regarding the importance of screening, leading to a disappointingly low incidence of early-stage diagnoses. As a result, a significant number of patients are diagnosed at later stages, frequently when peritoneal metastasis has already set in. Metastasis marks a critical turning point in gastric cancer, significantly worsening the prognosis to an average 5-year survival rate of less than 20% [3, 4]. The propensity for invasion and distant spread is a principal factor underlying the often disappointing outcomes of treatment efforts [5].

The National Cancer Institute reports that peritoneal metastasis is a prevalent destination for metastatic spread in various abdominal and pelvic cancers, notably gastric, pancreatic, colorectal, ovarian, and uterine malignancies, with the omentum identified as the predominant site for such metastases [6–8]. The peritoneal environment, rich in adipocytes, plays a critical role in the body's metabolic response by hydrolyzing fats to release fatty acids, glycerol, and other metabolic substrates into the circulation when energy demands arise [9]. These adipocytes are increasingly recognized for their active role in promoting the invasive and metastatic capabilities of several cancers such as ovarian and gastric cancers [8, 10]. Our previous investigation has elucidated that adipocytes can donate fatty acids (FAs) to GC cells, which in turn, facilitates the accumulation of lipid droplets (LDs). Subsequently, these LDs can be used to promote NADPH production via lipolysis and β-oxidation, endowing the cells with a survival advantage against anoikis [11]. LDs composed of a monolayer phospholipids encapsulating neutral lipids, predominantly triacylglycerol (TAG), are vital cellular energy stores. TAG consists of a glycerol backbone esterified with three fatty acids. However, most human cells are incapable of directly metabolizing glycerol, only specialized cells like adipocytes and hepatocytes possess glycerol kinase (GK), which converts glycerol to 3-phosphoglycerol (3-PG). For tumor cells, alternative metabolic routes are essential, such as the conversion of dihydroxyacetone phosphate (DHAP), a glycolytic intermediate, to 3-PG by glycerol-3-phosphate dehydrogenase 1/1-like (GPD1/1L), utilizing NADH as a cofactor. Hence, it is posited that GPD1/1L plays a significant role in the accumulation of LDs in GC cells. So, do lipid droplets serve functions beyond energy provision during the unanchored growth phase of peritoneal metastasis in gastric cancer cells?

In the context of peritoneal metastasis, GC cells undergo a state of unanchored growth, severed from the supportive extracellular matrix. This detachment is associated with an increased production of reactive oxygen species (ROS) [12, 13], which, when in excess, can inflict irreversible damage on cellular macromolecules, including proteins, lipids, and nucleic acids alike, thus significantly contributing to the onset of anoikis [14]. Iron, an indispensable element for cell growth and proliferation, is found in every mammalian cell. Notably, the convergence of ROS with ions can initiate a series of oxidative reactions that specifically target polyunsaturated fatty acids (PUFAs) in the cell membrane's phospholipids. The ensuing peroxidation leads to the disruption of the membrane's structural integrity, culminating in the induction of ferroptosis [15].

Ferroptosis is a type of programmed cell death that is distinct from other forms such as apoptosis, necrosis, and autophagy. It is characterized by the accumulation of ROS due to iron-dependent lipid peroxidation [16, 17]. The regulation of ferroptosis is governed by three principal pathways [18]: the cystine/GSH/the glutathione peroxidase 4 (GPX4) axis, which is central to cellular redox balance [19, 20]; the FSP1/CoQ10 axis, implicated in mitochondrial function [21, 22] and the GCH1/BH4/DHFR axis, which influences critical metabolic processes [23, 24]. Recent studies have shown a strong correlation between the progression of ferroptosis and lipid accumulation, particularly in the abundance of lipid droplets. Furthermore, these studies have revealed that FSP1 is predominantly localized to intracellular lipid droplets in adipocytes of brown adipose tissue [25]. However, the functional implications of this localization are not well understood. In this research, we found that the accumulation of lipid droplets in GC cells is associated with a reduction in FSP1 ubiquitination. This decrease in ubiquitination promotes ferroptosis resistance and significantly enhances the peritoneal metastatic potential of GC cells.

Materials and methods

Cell lines and reagents

Human GC cell lines were purchased from ATCC (Manassas, VA, USA). All cell lines were routinely cultured in RPMI-1640 medium (Hyclone, Cat No.SH30809.01), supplemented with 10% FBS and 1% penicillin/streptomycin solution, under a humidified atmosphere containing 5% CO_2. For suspension growth,

cells were plated on discs coated with poly-2-hydroxyethyl methacrylate (poly-HEMA) (Sigma, Cat No. P3932), prepared by dissolving poly-HEMA powder to a concentration of 12 mg/mL in 95% ethanol. To induce lipid droplets formation in GC cells, we employed oleic acid (OA) (Sigma, Cat No. O1383-1G) at a final concentration of 200μM. Additionally, the ferroptosis inducer RSL3 (Selleck, Cat No. S8155) and the FSP1 suppressor iFSP1 (Selleck, Cat No. S9663) were added to serum-free culture media.

CCK-8 cell viability

Detachment: 10,000 GC cells per well were cultured in a suspension culture within 96-well plates that had been coated with Poly-HEMA to induce anoikis. Subsequently, the cells were incubated in RPMI-1640 medium with Liproxstatin-1 (Lip-1, 2 μM, Selleck, Cat No.S7699) or Ferrostatin-1 (Fer-1, 2 μM, Selleck, Cat No.S7243) for a duration of 48 h.

Attachment: 5,000 GC cells per well were seeded in 96-well plates in advance. Subsequently, the cells were incubated in RPMI-1640 medium with RSL3 (Selleck, Cat No.S8155) or OA (200μM, Sigma, Cat No. O1383-1G) for 24 h, or with OA (200μM) alone for different time points.

To assess cell viability, 10 μL of the CCK-8 reagent (Corning Incorporated) was added to each well, followed by a 2 h incubation at 37 °C. The optical density (OD) at 450 nm was then measured using a microplate reader to quantify the cells' response to the treatment.

Immunofluorescence staining

GC cells were first fixed in 4% paraformaldehyde solution for 30 min, followed by permeabilization using a 0.5% Triton-X 100 solution in 1× PBS for 15 min. After permeabilization, the cells were blocked with a 5% BSA solution in 1× PBS for 1 h at room temperature to reduce non-specific binding. The cells were then incubated with primary antibodies against FSP1 (Proteintech, Cat No. 20886-1-AP) overnight at 4 °C. Subsequently, they were incubated with a secondary antibody, anti-rabbit IgG (Proteintech, Cat No. SA00013-4), diluted 1:200, for 1 h at room temperature. The cell nuclei were counterstained with DAPI (Biofroxx, Cat No. 1155MG010) at a final concentration of 1 μg/mL for 10 min. Lipid droplets were visualized using BODIPY 493/503 (Thermo Fisher Scientific, Cat No. D3922) for 15 min. After staining, the cells were washed with 1× PBS to remove excess stain and then sealed using an antifade reagent (Life Technologies, Cat No. P36934) to preserve fluorescence. Finally, the cells were observed under a fluorescence microscope.

Protein extraction and Western blotting

Protein lysates were extracted from cells using a radio-immunoprecipitation assay buffer (RIPA buffer, Beyotime, Cat No. P0013B), which is composed of 50 mM Tris-HCl at pH 7.4, 150 mM NaCl, 1% Triton X-100, 1% sodium deoxycholate, 1 mM EDTA, 0.1% SDS, and supplemented with Phenylmethanesulfonyl fluoride (PMSF) (Beyotime, Cat No. ST2573) to inhibit protease activity. The samples were centrifuged at 12,000 rpm at 4 °C for 10 min to collect the supernatants and the protein concentration of the lysates was determined using a bicinchoninic acid (BCA) protein assay kit (Beyotime, Cat No. P0012). Equal amounts of protein were then loaded onto sodium dodecyl sulfate–polyacrylamide gels for electrophoretic separation. Following electrophoresis, the proteins were transferred onto polyvinylidene fluoride (PVDF) membranes (Millipore, Cat No. IPVH00010). The membranes were incubated in 5% non-fat milk solution in 1× PBS for 1 h at room temperature and then, with primary antibodies overnight at 4 °C. Subsequently, Horseradish Peroxidase (HRP)-conjugated secondary antibodies (Proteintech Cat No. SA00001-1; Cat No. SA00001-2) were applied, and the immunoreactive signals were visualized using an enhanced chemiluminescence (ECL) detection reagent (Beyotime, Cat No. P0018FS) (Beyotime, Cat No. P0018FS) according to the established protocols. Quantifed the protein bands using Image J software after being normalized to the tublin level.

Lipidomics

Samples in liquid nitrogen were sent to Novogene Co., Ltd. (Beijing, China) for UHPLC-mass spectrum (MS)/MS analysis. Methanol (0.75 mL) was added to a 100 μL sample, which was placed into a glass tube with a Teflon lined cap, and the tube was vortexed. 2.5 mL of Methyl Tertiary Butyl Ether (MTBE) was added and the mixture was incubated for 1 h at room temperature in a shaker. Phase separation was induced by adding 0.625 mL of MS-grade water. Upon 10 min of incubation at room temperature, the sample was centrifuged at 1,000 g for 10 min. The upper phase was collected, and the lower phase was re-extracted with 1 mL of the solvent mixture (MTBE/methanol/water (10:3:2.5, v/v/v)), and collecting the upper phase. Combined organicphases were dried and dissolved in 100 μL of isopropanol for storage. Then analyzed by UHPLC-MS/MS using a Vanquish UHPLC system (Thermo Fisher, Germany) coupled with an Orbitrap Q ExactiveTM HF mass spectrometer (Thermo Fisher, Germany) in Novogene Co., Ltd. according to the established protocols.

Hematoxylin and eosin staining (H&E) and immunohistochemistry (IHC)

Fresh tumor tissue were fixed in 4% paraformaldehyde solution. Following fixation, the tissues underwent dehydration, paraffin embedding, and sectioning to prepare

for H&E staining or IHC analysis. The IHC was performed as described previously [11]. In brief, tissue sections were incubated with specific primary antibodies, including those against Ki-67 (Cell Signaling Technology Cat No. 9027s), diluted 1:500, and 4-Hydroxynonenal (4-HNE) (Abcam, Cat No. ab48506) diluted 1:400, overnight at 4 °C. The subsequent day, the slides were treated with corresponding secondary antibodies. The immunoreactivity was visualized using a 3,3'-diaminobenzidine (DAB) staining kit (ZSGB-BIO, Cat No. PV-9000). Images were captured randomly from each tumor section at a 200× magnification, with five images taken per tumor, using a Leica Aperio CS2 microscope.

Gene knockout mediated by CRISPR-Cas9

Using the services of AZENTA (Suzhou, China), we integrated single-guide RNAs (sgRNAs) and a CRISPR-Cas9 expression system into the lentiCRISPR-v2 vector. Subsequently, the generation of stable cell lines was achieved through antibiotic selection with 5 μg/mL puromycin (Sigma-Aldrich, USA), applied for a period of 3 days. Following this selection, single cells were sorted and seeded into 96-well plates for clonal expansion. These monoclonal populations were cultured for a duration of 3 to 4 weeks to allow for the establishment of stable cell lines. The efficiency of the gene knockout was subsequently validated through immunoblotting and quantitative polymerase chain reaction (qPCR) assays. The sequences of the sgRNAs targeting GPD1, GPD1L, and FSP1 were as follows: 5′-TCAGCCATCGCCAAGATCG T-3′ for GPD1, 5′-GCATAGACGAGGGCCCCGAG-3′ for GPD1L, and 5′-TCAAGGACAACTTCCGGCAG-3′ for FSP1, respectively.

Measurement of MDA, NADPH/NADP+ and GSH/GSSG

The relative malonaldehyde (MDA) concentration in cell was assessed using a lipid peroxidation MDA assay kit (Abcam Cat No. ab118970), according to the manufacturer's protocol. The determination of intracellular NADPH and total NADP levels were performed in accordance with the standard procedures provided by the manufacturer. For the measurement of GSH, a GSH/GSSG-Glo Assay Kit (Promega, #V6611) was employed, according to the manufacturer's instructions.

Anoikis and lipid ROS assay

Anoikis was induced by suspension culture. About 5×10^5cells were seeded in six-well plates pre-coated with poly-HEMA and cultured for 48 h. To assess cell viability, we employed a dual-staining method using calcein AM (Invitrogen, Cat No. C1430, 4 μM) and ethidium homodimer (EthD-1, Invitrogen, Cat No. E1169, 4 μM). Calcein AM serves as a green fluorescent marker for live cells, while EthD-1 indicates dead cells with red fluorescence. Both dyes were pre-incubated at 37 °C for 30 min before the cells were visualized under a fluorescence microscope to distinguish live from dead populations. For the lipid ROS assay, harvested cells were subjected to staining with C11 BODIPY 581/591 (Thermo Fisher Scientific, D3861), following the manufacturer's recommended protocol. The ROS levels were analyzed using a CytoFLEX cytometer instrument (Beckman Coulter, Brea) for flow cytometric analysis, and representative images were also captured using a fluorescence microscope for direct observation.

Adipocyte coculture

Adipocytes were extracted from high-fat diet mice which purchased from GemPharmatech Co., Ltd. Briefly, about 400 ~ 600 mg of adipose tissue was separated with forceps, washed twice with PBS in the culture dish, and the non-adipose tissue or blood vessels were removed. The tissue was cut with surgical scissors, transferred to a 50 ml sterile centrifuge tube, digested with 0.2% collagenase type I in a 37℃ shaker (80 ~ 100 rpm) for about 0.5 ~ 1 h. Digestion was terminated using 1640 medium containing 10% FBS and centrifuged at 1500 rpm for 5 min. The upper adipocytes were carefully collected using pipette tips and immediately used for coculture with GC cells after counting.

Animal studies

All animal experiments were approved by the Institutional Animal Care and Use Committee of Guangzhou Medical University. Female BALB/c nude mice, approximately 4 weeks of age, were purchased from Guangdong Medical Laboratory Animal Center (Foshan, China). We evaluated the peritoneal dissemination capacity of GC cells using an intraperitoneal injection model. Briefly, approximately 3×10^6 GC cells were enzymatically digested and resuspended in 400 μL of 1× PBS. This cell suspension was then immediately injected into the peritoneal cavity of each nude mouse, with five mice per experimental group. After a period of about one month, the mice were humanely sacrificed using the CO_2 asphyxiation. Subsequently, the peritoneum was meticulously examined and documented, and tissue samples were collected for subsequent embedding and histological staining analysis.

Statistical analyses

All experiments were repeated at least three times. Statistical p-values were obtained by application of the appropriate statistical analysis using the GraphPad Prism (version 8.0). Data were presented as the means ± standard deviation of the mean. To determine significant differences between two groups, we employed Student's t-test. For comparisons involving more than two groups,

we used one-way analysis of variance (ANOVA) and Tukey'stest for multiple comparisons. Statistical significance was considered as follows: $p < 0.05$ (*), $p < 0.01$ (**), $p < 0.001$ (***) and $p < 0.0001$ (****).

Results

Induction of ferroptosis by anchorage-independent growth in GC cells

Detachment of adherent cells can initiate a form of programmed cell death known as anoikis, a process in which ROS are notably implicated. This led us to investigate whether suspension growth could trigger ferroptosis in GC cells. Firstly, we cultured GC cells in a state of suspension using dishes coated with poly-HEMA. Our findings revealed that compared to anchorage, detached BGC823, SGC7901, AGS and HGC27 cells exhibited decreased intracellular NADPH and GSH production (Fig. 1A). Interestingly, staining with C11 BODIPY 581/591 revealed a significant elevation in intracellular lipid peroxidation levels in suspended GC cells (Fig. 1B and C). Additionally, MDA, a lipid peroxidation marker, demonstrated a significant increase in the detached GC cells (Fig. 1D). Meanwhile, cell death was assessed using a LDH detection kit and calcein AM/EthD-1 staining. Our findings demonstrated a significant enhancement in LDH release (%) (Fig. 1E) and cell death in the suspended GC cells (Fig. 1F and G). Furthermore, we confirmed that the ferroptosis inhibitors Lip-1 and Fer-1 effectively mitigated the cell death of GC cells during suspension culture (Fig. 1H). In our study, we demonstrate that anchorage-independent growth is a potent inducer of ferroptosis. Moreover, our findings reveal that inhibiting ferroptosis significantly enhances the suspension growth capabilities of gastric cancer cells.

Lipids droplets attenuate ferroptosis in GC cells during suspension growth

Specific alterations in the lipid metabolism, including increased fatty acid uptake and synthesis, are recognized as a mechanism that contribute to anoikis resistance in various types of cancers. Consistent with this, we observed a significant accumulation of neutral lipids in lipid droplets of BGC823 and SGC7901 cells after suspension culture, as visualized by the fluorescent sensor BODIPY 493/503 (Fig. 2A). Importantly, the level of TAG markedly increased after suspension culture (Fig. 2B). Next, we employed lipid mass spectrometry to analyze the changes in the distribution of FAs across different lipid species. Specifically, the intracellular PUFAs were predominantly found in TAG, with a comparatively lower presence in phospholipids (Fig. 2C and Figure S1A). Collectively, these findings suggested that LDs may play a role in mitigating lipid peroxidation. We then induced LDs accumulation in GC cells by co-culturing GC cells with OA or adipocytes (Figure S1B). Our findings indicated that the significant increase in cell death and lipid ROS levels, occurred after suspension culture, was mitigated by OA or adipocytes (Fig. 2D-F). In addition, employing antibodies specific to 4-HNE, a marker of lipid peroxidation, we observed an elevation in lipid peroxidation after suspension culture, which was attenuated by OA treatment (Fig. 2G). Furthermore, under adherent culture conditions, we used the GPX4 inhibitor RSL3 to induce ferroptosis in GC cells. Both OA and adipocytes were found to inhibit ferroptosis induced by RSL3 (Fig. 2I and Figure S1C), as well as lipid ROS levels (Fig. 2H). Additionally, OA provided protection against death induced by arachidonic acid (AA), a PUFAs (Figure S1D). Collectively, these results demonstrate the role of lipids drolets in attenuating ferroptosis in GC cells during suspension growth.

GPD1/1L mediated lipid droplets accumulation confers ferroptosis resistance

Triacylglycerols serve as the predominant molecules of energy storage in mammalian cells and are responsible for lipid droplets formation. To elucidate the enzymatic pathways that facilitate the incorporation of both endogenous and exogenous fatty acids into lipid droplets, we first examined several key enzymes involved in triglyceride synthesis. These included GPD1 and GPD2, which are isoforms of the rate-controlling enzyme for glycerol-3-phosphate formation, glycerol-3-phosphate dehydrogenase 1 like protein (GPD1L), lysophosphatidyl acyltransferase 1 (AGPAT1) and diacylglycerol acyltransferase 1 and 2 (DGAT1 and DGAT2). Interestingly, under the suspension culture condition, we observed significant upregulation of GPD1 and GPD1L in BGC823 and SGC7901 cells (Fig. 3A). In addition, treatment with 200 μM OA induced a time-dependent increase in GPD1 and GPD1L protein expression in BGC823, SGC7901, AGS and HGC27 cells (Fig. 3B). Subsequent gene set enrichment analysis (GSEA) of transcriptome sequencing data from 375 GC patients in the TCGA database revealed that pathways related to fatty acid metabolism were significantly enriched in the high-expression groups of GPD1 or GPD1L (Figure S2A and B).

To investigate the necessity of GPD1 and GPD1L for lipid droplet accumulation, we generated SGC7901 and HGC27 cell lines with double knockout (DKO) of GPD1 and GPD1L using CRISPR/Cas9 systerm. We successfully established two independent cell lines with strong loss-of-function phenotypes and confirmed that the DKO of GPD1 and GPD1L was less effective in promoting triglyceride synthesis and lipid droplet formation under suspension culture conditions. Even with attachment and the presence of exogenous OA, triglyceride synthesis and lipid droplet formation remained diminished in these

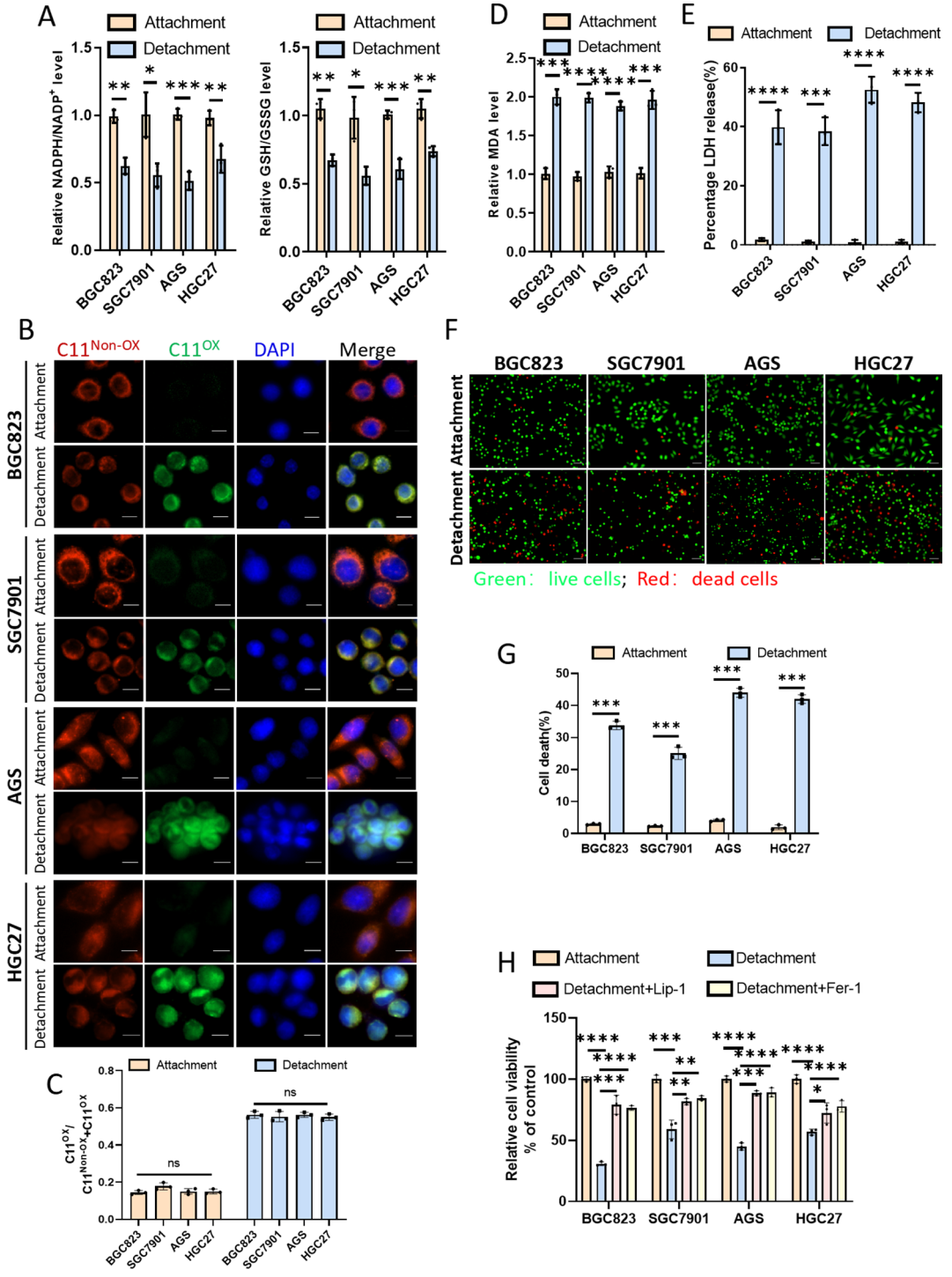

Fig. 1 Induction ferroptosis by anchorage-independent growth in GC cells. **A** Measurement of NADPH/NADP$^+$ and GSH/GSSG levels in the GC cells under attached and detached conditions. **B** Lipid peroxidation in GC cells was assessed under attached and detached conditions using a fluorescence microscope to measure the fluorescence intensity of C11 BODIPY 581/591. Red fluorescence represents $C11^{Non\text{-}OX}$ and green fluorescence represents $C11^{OX}$. Cell nuclei were stained with DAPI. Scale bars 10 μm. **C** Quantification of the ratios of $C11^{OX}$ in the GC cells under attached and detached conditions. **D** Measurement of MDA levels in GC cells under attached and detached conditions. **E** Measurement of LDH levels in GC cells under attached and detached conditions. **F**, **G** Representative images and quantification of GC cells under attached or detached conditions for 48 h. Scale bars 50 μm. Calcein AM (green fluorescent dye) was used to detect cell viability and EthD-1 (red fluorescent dye) for cell death. **H** Cell viability assessment in GC cells under attached or detached conditions, with or without exposure to ferroptosis inhibitor Lip-1 or Fer-1. Data are mean ± SD of at least three replicates from two independent experiments. P values were determined by a two-tailed t-test.

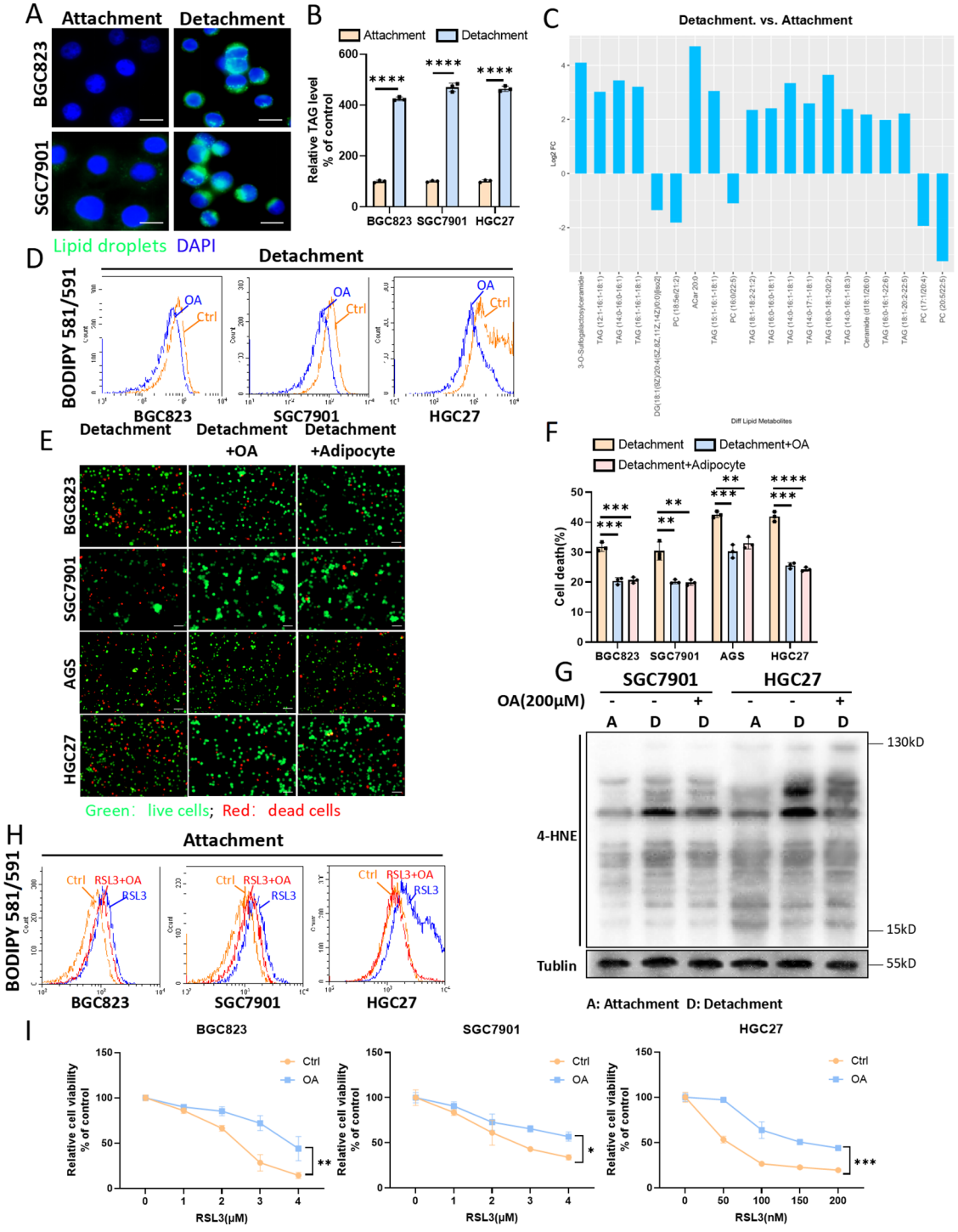

Fig. 2 Lipids drolets attenuate ferroptosis in GC cells during suspension growth. **A** BODIPY 493/503 imaging of neutral lipid accumulation (green) in BGC823 and SGC7901 under detached conditions. Cell nuclei were stained with DAPI. Scale bars 10 μm. **B** Measurement of TAG levels in the GC cells under attached and detached conditions. **C** Fold change in the distribution of PUFAs in various lipid contents (log2) of cells cultured with attachment and detachment detected by lipid mass spectrometry. **D** Analysis of lipid ROS using BODIPY 581/591 by flow cytometry in GC cells under detached conditions and treated with OA (200 μM). **E**, **F** Representative images and quantification of GC cells treated with OA (200 μM) or co-cultured with adipocytes under detached conditions for 48 h. Scale bars 50 μm. Calcein AM (green fluorescent dye) was used to detect cell viability and EthD-1 (red fluorescent dye) for cell death. **G** 4-HNE expression detected by western blot analysis in GC cells treated with OA (200 μM) under detached conditions. **H** Analysis of lipid ROS using C11 BODIPY 581/591 by flow cytometry in GC cells under attached conditions treated with RSL3. **I** Cell viability of indicated GC cells treated with RSL3 for 24 h. Data are mean ± SD of at least three replicates from two independent experiments. P values were determined by a two-tailed t-test.

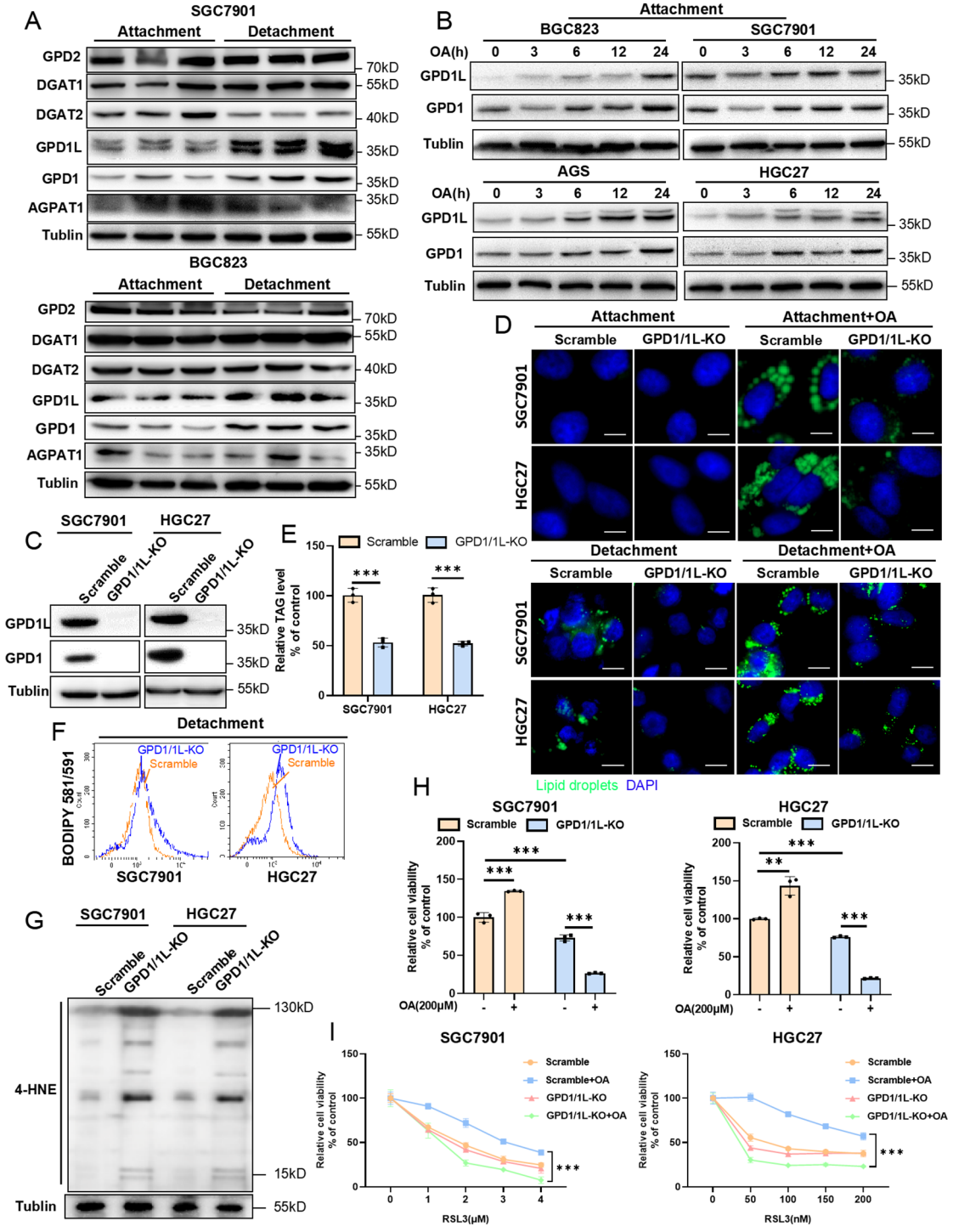

Fig. 3 GPD1/1L mediated lipid droplets accumulation confers ferroptosis resistance. **A** Key enzymes related to lipid synthesis detected by western blot in the GC cells under attached or detached conditions. **B** Western blot analysis of GPD1 and GPD1L expression in GC cells treated with OA (200 μM) for 3 h, 6 h, 12 h and 24 h under attached conditions. **C** The effect of gRNAs-mediated gene knockout of GPD1 and GPD1L in SGC7901 and HGC27 cells was confirmed by western blot analysis. **D** BODIPY 493/503 imaging of neutral lipid accumulation (green) in the indicated GC cells under attached or detached conditions and treated with OA (200 μM). Cell nuclei were stained with DAPI. Scale bars 10 μm. **E** Measurement of TAG levels in the indicated GC cells under detached conditions. **F** Analysis of lipid ROS using C11 BODIPY 581/591 by flow cytometry in the indicated GC cells under detached conditions. **G** 4-HNE expression detected by western blot analysis in the indicated GC cells under detached conditions. **H** Comparison of viability of the GPD1/1L knockout GC cells treated with OA (200 μM) under detached conditions for 48 h as revealed by CCK8 assays. **I** Cell viability of the indicated GC cells treated with OA (200 μM) and treated with RSL3 for 24 h. Data are mean ± SD of at least three replicates from two independent experiments. P values were determined by a two-tailed t-test.

lines (Fig. 3C and D). Importantly, the level of TAG markedly decreased after suspension culture (Fig. 3E). Moreover, the DKO of GPD1 and GPD1L resulted in higher levels of lipid peroxidation and its end products 4-HNE during suspension growth (Fig. 3F and G). Importantly, the DKO cells exhibited a significant reduction in the protective effect of OA on cell viability (Fig. 3H and I). Additionally, the SGC7901 or HGC27 GPD1/1L-DKO cell lines displayed a slight increase in sensitivity to the ferroptosis inducer RSL3. Therefore, these findings underscore the importance of GPD1 and GPD1L in lipid droplet formation and their role in modulating GC cell resistance to ferroptosis.

Accumulated lipid droplets suppress the ubiquitination of FSP1

The data presented above demonstrate that lipid droplets confers ferroptosis resistance in GC cells. Ferroptosis, a form of regulated cell death driven by iron-dependent lipid peroxidation, can be antagonized by several proteins, including GPX4, ferroptosis inhibitory protein 1 (FSP1), and dihydroorotate dehydrogenase (DHODH). To identify the key pathway responsible for this resistance in GC cells, we analyzed the expression levels of SLC7A11, FSP1, DHODH and GPX4 proteins and observed a significant upregulation of FSP1 in response to OA or adipocyte co-culture. However, the elevation of GPX4 expression was not significant (Fig. 4A and Figure S3A). Furthermore, FSP1 upregulation induced by OA was not observed in the DKO of GPD1/1L cell lines (Figure S3B). Interestingly, using confocal microscopy, we detected the localization of FSP1 and discovered that its expression was up-regulated after OA treatment, with a subset of FSP1 localizing to the lipid droplet surface (Fig. 4B and C). These findings indicate FSP1's role in conferring resistance to ferroptosis in GC cells.

To ascertain whether lipid droplets exert a direct influence on the transcript levels of FSP1, thereby modulating its protein expression, we performed qPCR assays. The qPCR data indicated that the FSP1 mRNA levels remained largely unaltered in GC cells harboring lipid droplets (Fig. 4D). Given the critical role of ubiquitination in protein degradation, we employed the protein synthesis inhibitor cycloheximide (CHX, 200 μg/mL) and the proteasome inhibitor MG132 (20 μM) to explore FSP1 ubiquitination. Treatment with CHX led to a diminution in FSP1 protein levels (Fig. 4E), while MG132 treatment resulted in an increase FSP1 protein level (Fig. 4F). Notably, pre-treatment with OA prior to CHX addition caused a significant increase of FSP1 protein (Fig. 4G). Immunodetection with pan-ubiquitin antibodies revealed a marked reduction in FSP1 ubiquitination in OA-induced lipid droplet-containing GC cells (Fig. 4H). Collectively, These outcomes suggest that lipid droplets may suppress the ubiquitination of FSP1, consequently attenuating its proteasomal degradation.

Suppression of FSP1 enhances ferroptosis in GC cells

To ascertain the role of FSP1 in regulating lipid peroxidation during the suspension growth of GC cells, we initiated experiments using the FSP1 inhibitor iFSP1. Our findings demonstrate that FSP1 inhibition during suspension culture significantly abrogated the OA induced ferroptosis resistance in GC cells (Fig. 5A). FSP1 knockout in the cell lines was validated through western blot (Fig. 5B). Furthermore, the FSP1 knockout cell lines exhibited elevated lipid peroxidation levels and the end product of lipid peroxidation during suspension growth, which corresponded with a decreased cell viability (Fig. 5C-E). Additionally, these cell lines exhibited a pronounced increase in sensitivity to RSL3 induced ferroptosis under attached condition (Fig. 5F). Consistent with our hypothesis, under conditions that induce ferroptosis, as triggered by RSL3 in FSP1 knockout GC cells, OA failed to enhance cell viability (Fig. 5G). To further elucidate the impact of FSP1, we constructed cell lines overexpressing FSP1, and the overexpression was confirmed by western blotting (Fig. 5H). These FSP1-overexpressing cell lines displayed enhanced cell viability (Fig. 5I), along with reduced lipid peroxidation levels during suspension growth (Fig. 5J) and decreased sensitivity to RSL3-induced ferroptosis under attached conditions (Fig. 5K). These results demonstrate ferroptosis is exacerbated in GC cells when FSP1 is suppressed.

Knockout FSP1 reduces the peritoneal dissemination of GC cells in vivo

Subsequently, we explored the role of FSP1 in peritoneal dissemination in vivo. Both knockout and control GC cells were injected into the peritoneal cavities of nude mice. FSP1 knockout significantly diminished the formation of mesenteric metastatic nodules on the intestinal wall of the mice (Fig. 6A). Histological examination using H&E staining and IHC revealed that the absence of FSP1 led to a reduction of Ki-67 levels, indicative of decreased cell proliferation, while there was a concomitant increase in 4-HNE levels, which is consistent with our prior in vitro findings (Fig. 6B).

Discussion

In clinical practice, GC patients with mesenteric metastasis pose a significant challenge due to the scarcity of effective treatment options and generally poor outcomes. The phenomenon of anoikis resistance is a key determinant in the metastatic progression of numerous malignancies, including GC. Anoikis, a specialized form of apoptosis, is triggered when cells detach from the extracellular matrix. It represents a pivotal barrier to tumor metastasis, as

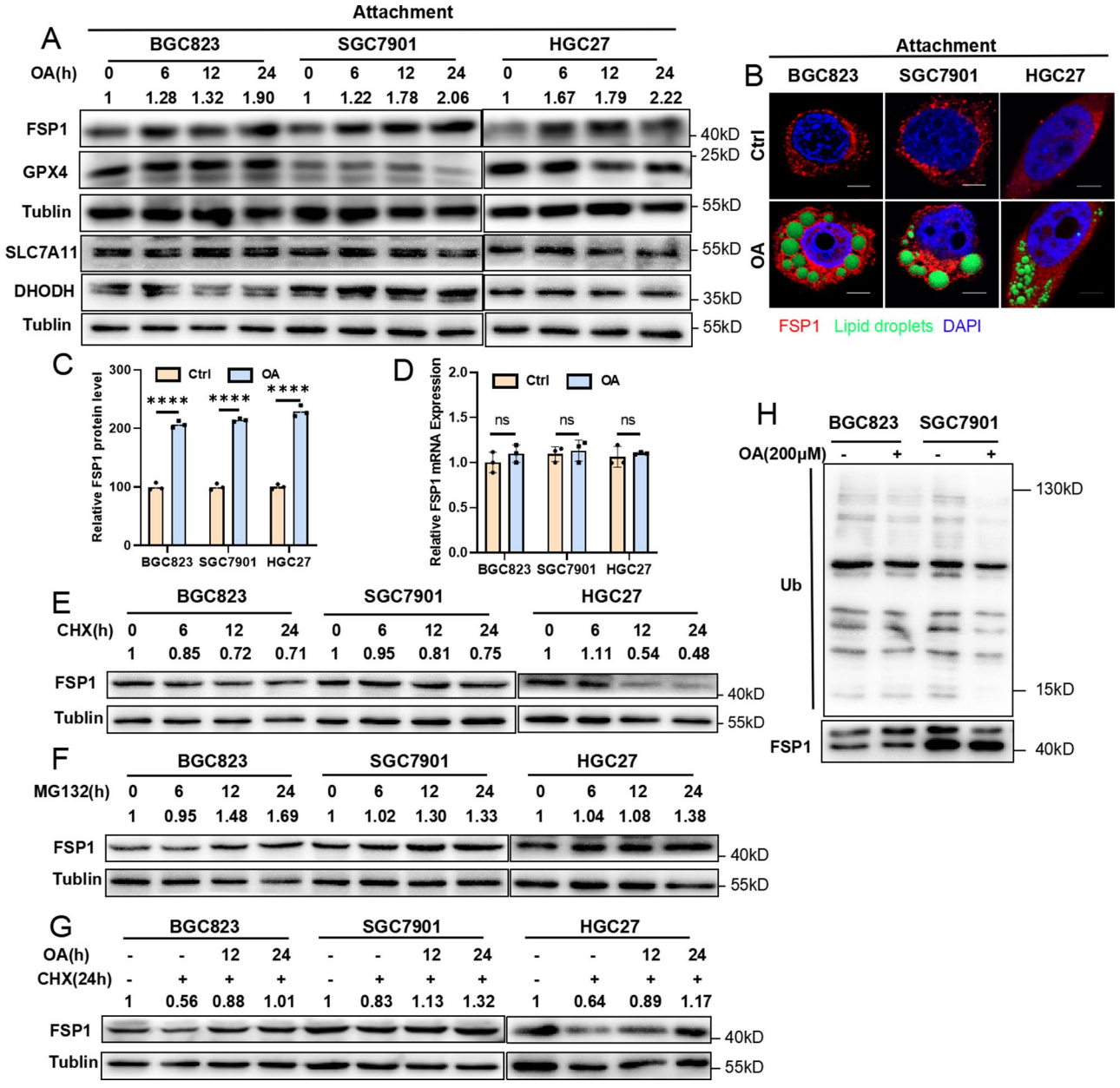

Fig. 4 Accumulated lipid droplets suppress the ubiquitination of FSP1. **A** Key proteins related to ferroptosis regulatory detected by western blot in the GC cells treated with OA (200μM) for 6 h, 12 h and 24 h. **B** Confocal imaging of distribution of FSP1 (red) and lipid droplets (green) in GC cells treated with (200μM) for 24 h. Cell nuclei were stained with DAPI. Scale bars 5 μm. **C** Quantification of FSP1 expression in GC cells. Each data point represents the fluorescence intensity signal from an independent biological replicate ($n = 3$). **D** The expression of FSP1 in gastric cancer cells treated with was analyzed by qPCR treated with OA (200 μM) for 24 h. GAPDH as the loading reference control. **E**, **F** Western blot analysis of FSP1 expression in GC cells treated with CHX (200 μg/ml) or MG132(20 μM) for 6 h, 12 h and 24 h. **G** Western blot analysis of FSP1 expression in GC cells treated with CHX (200 μg/ml) for 24 h and OA (200 μM) for 12 h and 24 h. **H** IP analysis demonstrating the ubiquitination level of FSP1 in GC cells treated with OA (200 μM) for 24 h. Data are mean ± SD of at least three replicates from two independent experiments. P values were determined by a two-tailed t-test.

cells must evade this programmed cell death to successfully colonize distant sites [26, 27]. Anoikis resistance is essential for the survival and sustained propagation of metastatic tumor cells [28]. Among the myriad of factors implicated in the induction of anoikis, the metabolic perturbations that lead to a critical surge in ROS are particularly significant. These ROS, when influenced by iron ions, have the capacity to assail the polyunsaturated fatty acids within the cell membrane. This assault initiates a cascade of lipid peroxidation events, which are diagnostic of ferroptosis. The potential interplay between anoikis and the onset of ferroptosis is a compelling avenue for further research. Decoding this nexus is crucial as it promises to deepen our comprehension of the intricate

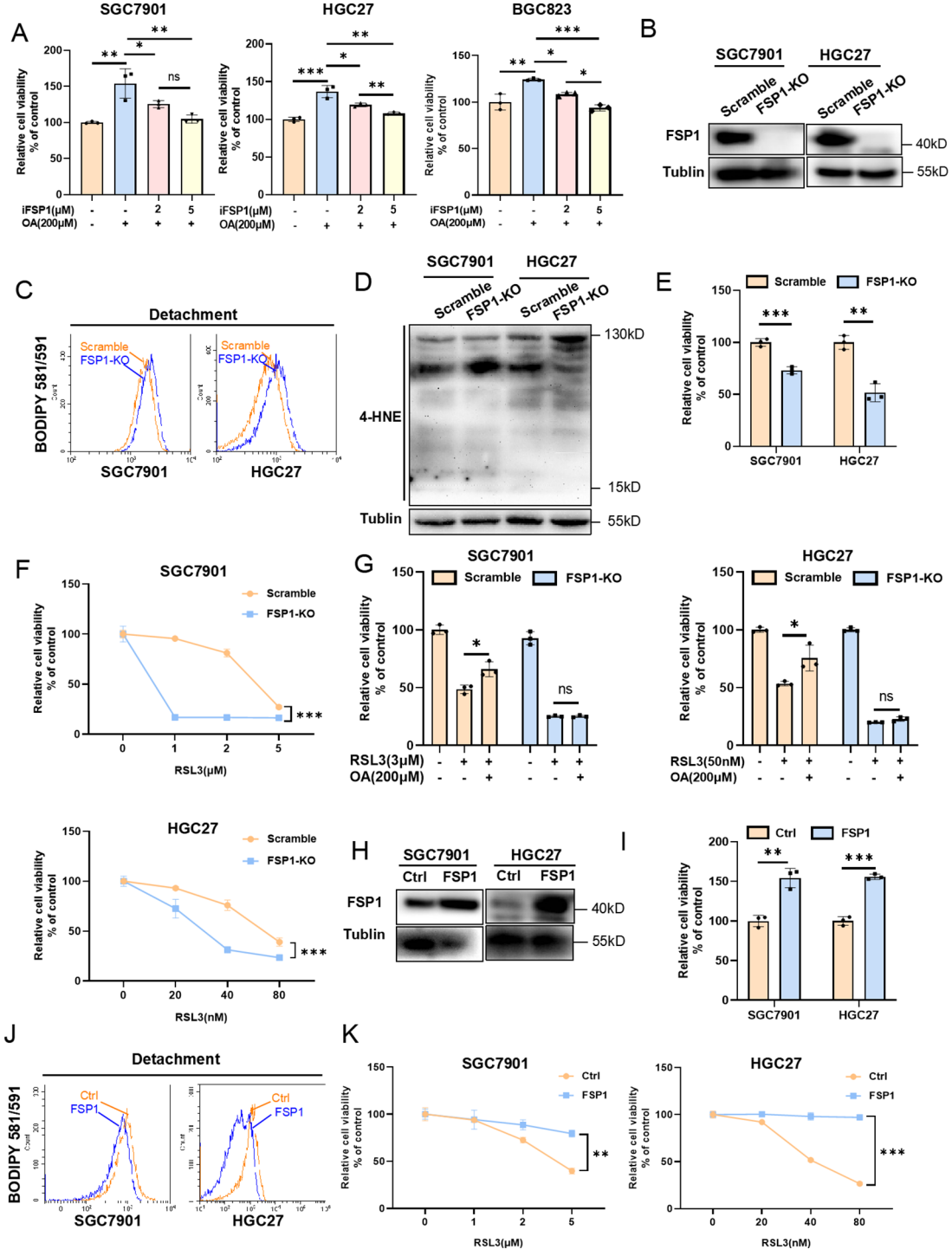

Fig. 5 Suppression of FSP1 enhances ferroptosis in GC cells. **A** Cell viability of indicated GC cells treated with different concentrations of iFSP1 and OA(200 μM) for 24 h under detached conditions. **B** The effect of gRNAs-mediated gene knockout of FSP1 in SGC7901 and HGC27 cells was confirmed by western blot. **C** Analysis of lipid ROS using C11 BODIPY 581/591 by flow cytometry in the indicated GC cells under detached conditions. **D** 4-HNE expression detected by western blot analysis in the indicated GC cells under detached conditions. **E** Comparison of viability of the FSP1 knockout GC cells under detached conditions for 48 h as revealed by CCK8 assays. **F** Cell viability of indicated GC cells treated with different concentrations of RSL3 for 24 h as revealed by CCK8 assays. **G** Cell viability measured by CCK-8 assay of the indicated GC cells treated with OA (200 μM) and treated with RSL3 for 24 h. **H** The effect of overexpressing FSP1 in SGC7901 and HGC27 cells was confirmed by western blot. **I** Comparison of viability of the overexpressing FSP1 GC cells under detached conditions for 48 h as revealed by CCK8 assays. **J** Analysis of lipid ROS using C11 BODIPY 581/591 by flow cytometry in the indicated GC cells under detached conditions. **K** Cell viability of indicated GC cells treated with RSL3 for 24 h. Data are mean ± SD of at least three replicates from two independent experiments. P values were determined by a two-tailed t-test.

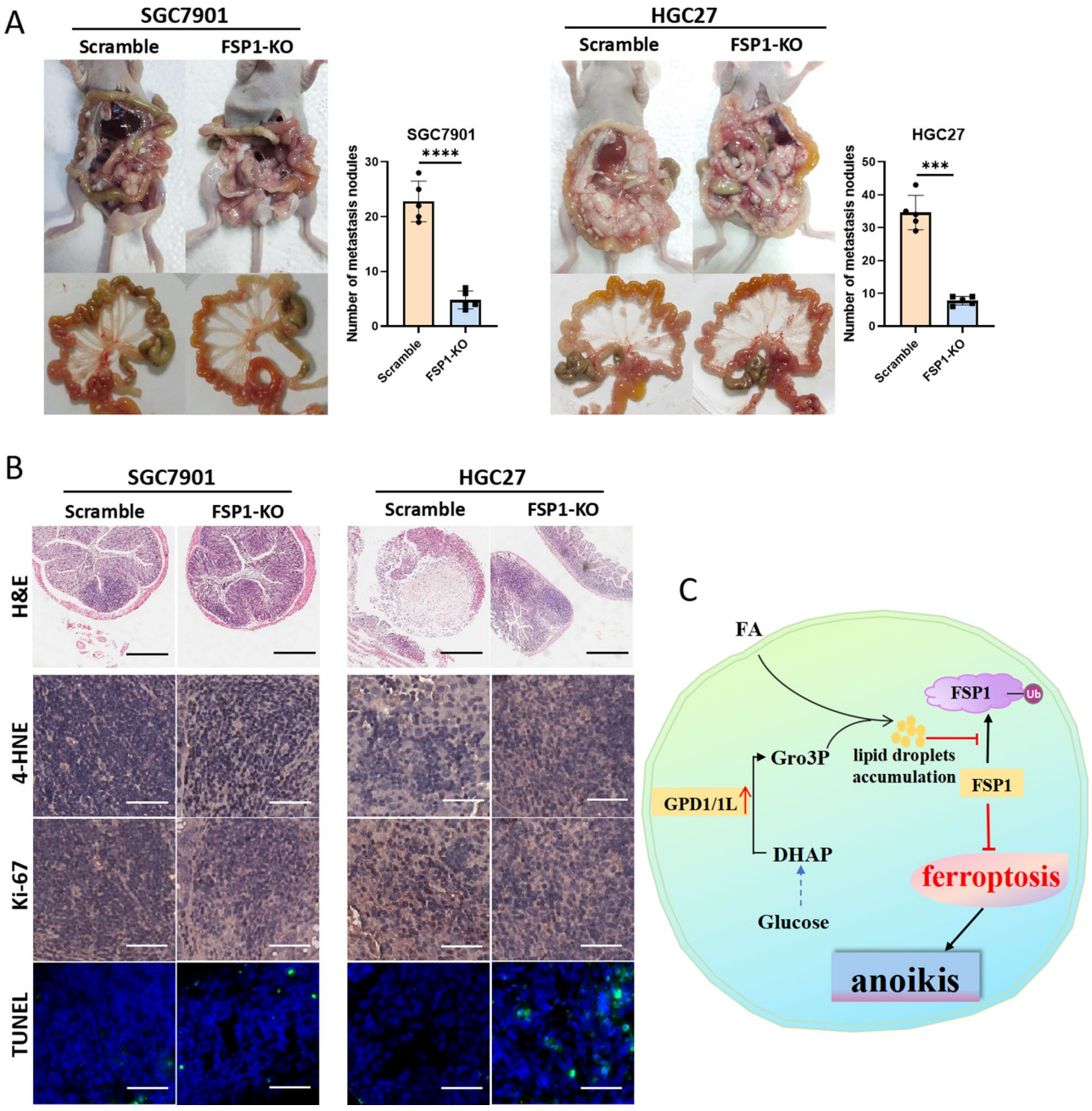

Fig. 6 Knockout FSP1 reduces the peritoneal dissemination of GC cells in vivo. **A** Nude mice were intraperitoneally injected with either scramble control or FSP1-KO of the described GC cells. After approximately one month, the mice were examined for metastases in the abdomen and the affected areas were photographed. The metastatic lesions in the intestines were quantified and presented in a histogram for every group ($n = 5$). **B** Histological analysis of dispersed tumors in the nude mice included H&E staining (scale bars 0.5 mm), 4-HNE (scale bars 50 μm) and Ki67. scale bars 50 μm). **C** Proposed mechanism of FSP1 action in the inhibition of ferroptosis. GPD1/1L regulates the accumulation of lipid droplets and can suppress the ubiquitination of FSP1. This inhibition may confer resistance to ferroptosis, thereby further suppressing the process of anoikis in GC cells. Apoptotic cells within the tumors were visualized by TUNEL staining (green), with nuclei counter stained by DAPI (blue) (scale bars 50 μm).

pathways of cell death and may reveal innovative therapeutic strategies for conditions marked by abnormal cell detachment and the advancement of tumors. In this study, we revealed that anchorage-independent growth of GC cells potently induced ferroptosis, which can be effectively mitigated by the ferroptosis inhibitors. Our findings substantiate that detachment from the extracellular matrix triggers ferroptosis in GC cells.

Exogenous metabolites including lipids are potent modulators of cell function and fate. Our previous study demonstrated that peritoneum-derived adipocytes induces robust lipid droplets accumulation in GC cells.

However, the pathways that drive lipid droplet accumulation in GC cells and the relationship between lipid droplets and ferroptosis is complicated. Bailey et al. [29] have reported that lipid droplets protected Drosophila glial cell niche and neural stem cells from damaging PUFAs peroxidation. The accumulation of excess free fatty acids (FFAs) can induce oxidative stress and mitochondrial dysfunction, resulting in the overproduction of ROS, accumulation of unsaturated fatty acids, and escalation of lipid peroxidation [30]. Therefore, tumor cells should aim to minimize oxidative phosphorylation and reduce ROS production, especially during the process of metastasis.

Here, we have demonstrated that lipid droplets derived from OA treatment or coculture with adipocytes, can significantly attenuate ferroptosis in GC cells during suspension growth. This indicates that lipid droplets play a significant role in ferroptosis resistance and the development of peritoneal metastasis in GC cells.

Moving forward, our investigation is focused on identifying and characterizing the pivotal enzymes that orchestrate the biogenesis of lipid droplets in GC cells. The synthesis of triglycerides, a critical lipid class in lipid droplets, is contingent upon the availability of glycerol-3-phosphate(G3P), a key precursor that is requisite for the esterification process irrespective of the fatty acid's origin, be it exogenous or endogenous. G3P is the basic unit of various lipid metabolites, further serving as the backbone for lipid biosynthesis and different signaling molecules, participating in regulating biological processes of cell survival, energy metabolism, and oxidative stress [31, 32]. GPD1 and GPD1L share 70% of the same protein sequence and catalyze the same function. They utilize NADH as a coenzyme to catalyze the production of dihydroxyacetone phosphate derived from glucose to G3P in the cytoplasm. Interestingly, emerging evidence indicates that GPD1 plays a tumor-promoting role [33]. and GPD1/GPD1L DKO in mouse kidney cancer cells inhibited lipid synthesis and in vitro/ in vivo tumor growth [34]. An observational bladder cancer study also suggested correlated increases in GPD1 and fatty acid synthetic enzyme activities in tumor tissues [35]. In our investigation, we observed that GPD1/1L utilize intracellular unsaturated fatty acids to synthesize triglycerides during the process of detachment, leading to the accumulation of these lipids within cells during the early stages of metastasis. This results in a reduction lipid peroxidation and preventing ferroptosis. Particularly, when GC cells are transferred to the adipocyte-rich peritoneal environment, the expression of cytoplasmic GPD1/1L is significantly upregulated. This upregulation leads to the accumulation of lipid droplets, potentially facilitating tumor progression. Elucidating the precise scope of GPD1's tumor-promoting roles will necessitate additional research.

The system Xc-/GSH/GPX4 axis is a GSH-dependent ferroptosis defense system and is one of the most important antioxidant systems for ferroptosis resistance [36]. However, in some cell types or cell lines, inhibition of GPX4 cannot induce ferroptosis, which indicates the presence of alternative mechanisms. Among them, the GSH-independent coenzyme Q oxidoreductase FSP1 acts in parallel with GPX4, representing another major regulator of ferroptosis [21, 22]. FSP1, as one of the main regulatory molecules of ferroptosis [37] is regulated by upstream factors, including transcription factors and noncoding RNA, and is subject to epigenetic modifications, which affect the progress of FSP1-related diseases [38]. FSP1 is closely associated with the poor prognosis of malignant tumors and plays an important role in disease treatment [39]. Moreover, a study found that dehydroabietic acid can stimulate the upregulation of FSP1 through activating NRF2 pathway, inhibit ROS accumulation and lipid peroxidation, and mitigate nonalcoholic fatty liver disease (NAFLD) induced by a high-fat diet (HFD) [40]. In our investigation, we found that lipid droplets, when accumulated, can suppress the ubiquitination of FSP1. This observation lays the groundwork for delving into novel molecular mechanisms, particularly from the perspective of protein stability pathway.

Briefly, when exposed to a high-fat environment in the peritoneum, a large amount of fatty acids are taken up for synthesis of triglycerides, which can upregulate FSP1 to eliminate intracellular lipid ROS during metastasis. This study unveils the important relationship between lipid metabolism reorganization and ferroptosis, demonstrating that GPD1/1L regulates the accumulation of lipid droplets and that lipid droplets can confer resistance to ferroptosis through FSP1(Fig. 6C). These findings provide a novel target for the prevention and treatment of peritoneal metastasis of gastric cancer.

Limitations of the study

Our study has certain limitations that should be addressed in future research. Firstly, it would be beneficial to include a comparative analysis of the effects of various inhibitors on cells to further substantiate the claim that ferroptosis significantly contributes to cell death upon detachment. Additionally, while our in vitro experiments have shown that lipid droplets can confer resistance to ferroptosis through FSP1, it is crucial to validate these findings through in vivo studies. Therefore, we intend to employ a range of inhibitors to investigate cell death and conduct in vivo experiments to confirm the role of FSP1 in ferroptosis. This approach will provide a more comprehensive understanding of the mechanisms involved and strengthen our conclusions regarding the significance of ferroptosis in cell death processes.

Supplementary Information

The online version contains supplementary material available at https://doi.org/10.1186/s12964-025-02126-x.

Supplementary Material 1

Supplementary Material 2

Supplementary Material 3

Acknowledgements

This work was supported by the Natural Science Foundation of China (grant numbers 82173141, 81702886), Bureau of Education of Guangzhou Municipality (grant number 202032801), the Education Department of Guangdong Province (grant numbers 2021ZDZX2044 and 2019KZDXM058), the Education Department of Guangzhou Medical University (grant numbers 2021A090), the scientific research project of Traditional Chinese Medicine Bureau of Guangdong Province (grant numbers 20222122), the scientific research capacity improvement project of 2023 from Guangzhou Medical University, and the open research funds (2021) and the funds of selected project (2022) from GMU-GIBH Joint School of Life Sciences, Guangzhou Medical University. The funders had no roles in the design of the study, data collection, analysis, interpretation, or decision to write and publish the work.

Author contributions

S. Li and H. Su: Conceived and designed the research. G. Lin, Q. Liu, C. Xie, K. Ding, G. Mo, L. Zeng, F. Zhang, R. Liu, L. Lu, W. Hong and Y. Mao: Performed the research and acquired the data. G. Lin, Q. Liu, S. Li and H. Su: Analyzed and interpreted the data. G. Lin, Q. Liu, S. Li and H. Su: Involved in drafting and revising the manuscript. All authors read and approved the final manuscript.

Funding

This work was supported by the Natural Science Foundation of China (grant numbers 82173141, 81702886), Bureau of Education of Guangzhou Municipality (grant number 202032801), the Education Department of Guangdong Province (grant numbers 2021ZDZX2044 and 2019KZDXM058), the Education Department of Guangzhou Medical University (grant numbers 2021A090), the scientific research project of Traditional Chinese Medicine Bureau of Guangdong Province (grant numbers 20222122), the scientific research capacity improvement project of 2023 from Guangzhou Medical University, and the open research funds (2021) and the funds of selected project (2022) from GMU-GIBH Joint School of Life Sciences, Guangzhou Medical University. The funders had no roles in the design of the study, data collection, analysis, interpretation, or decision to write and publish the work.

Data availability

No datasets were generated or analysed during the current study.

Declarations

Ethical approval

All animal experiments were approved by the Institutional Animal Care and Use Committee of Guangzhou Medical University.

Competing interests

The authors declare no competing interests.

Received: 18 November 2024 / Accepted: 24 February 2025
Published online: 12 March 2025

References

1. Smyth EC, Nilsson M, Grabsch HI, van Grieken NC, Lordick F. Gastric cancer. Lancet. 2020;396(10251):635–48.
2. Sung H, Ferlay J, Siegel RL, Laversanne M, Soerjomataram I, Jemal A, Bray F. Global Cancer statistics 2020: GLOBOCAN estimates of incidence and mortality worldwide for 36 cancers in 185 countries. CA Cancer J Clin. 2021;71(3):209–49.
3. Correa P. Gastric cancer: overview. Gastroenterol Clin North Am. 2013;42(2):211–7.
4. Santoro R, Ettorre GM, Santoro E. Subtotal gastrectomy for gastric cancer. World J Gastroenterol. 2014;20(38):13667–80.
5. Coffey JC, Dillon M, Sehgal R, Dockery P, Quondamatteo F, Walsh D, Walsh L. Mesenteric-Based surgery exploits gastrointestinal, peritoneal, mesenteric and fascial continuity from duodenojejunal flexure to the anorectal Junction–A review. Dig Surg. 2015;32(4):291–300.
6. Gerber SA, Rybalko VY, Bigelow CE, Lugade AA, Foster TH, Frelinger JG, Lord EM. Preferential attachment of peritoneal tumor metastases to omental immune aggregates and possible role of a unique vascular microenvironment in metastatic survival and growth. Am J Pathol. 2006;169(5):1739–52.
7. Berek JS, Renz M, Kehoe S, Kumar L, Friedlander M. Cancer of the ovary, fallopian tube, and peritoneum: 2021 update. Int J Gynaecol Obstet. 2021;155(1):61–85.
8. Nieman KM, Kenny HA, Penicka CV, Ladanyi A, Buell-Gutbrod R, Zillhardt MR, Romero IL, Carey MS, Mills GB, Hotamisligil GS, et al. Adipocytes promote ovarian cancer metastasis and provide energy for rapid tumor growth. Nat Med. 2011;17(11):1498–503.
9. Luo L, Liu M. Adipose tissue in control of metabolism. J Endocrinol. 2016;231(3):R77–99.
10. Tan Y, Lin K, Zhao Y, Wu Q, Chen D, Wang J, Liang Y, Li J, Hu J, Wang H, et al. Adipocytes fuel gastric cancer omental metastasis via PITPNC1-mediated fatty acid metabolic reprogramming. Theranostics. 2018;8(19):5452–68.
11. Li S, Wu T, Lu YX, Wang JX, Yu FH, Yang MZ, Huang YJ, Li ZJ, Wang SL, Huang L, et al. Obesity promotes gastric cancer metastasis via Diacylglycerol acyltransferase 2-dependent lipid droplets accumulation and redox homeostasis. Redox Biol. 2020;36:101596.
12. Kamarajugadda S, Cai Q, Chen H, Nayak S, Zhu J, He M, Jin Y, Zhang Y, Ai L, Martin SS, et al. Manganese superoxide dismutase promotes Anoikis resistance and tumor metastasis. Cell Death Dis. 2013;4(2):e504.
13. Li AE, Ito H, Rovira II, Kim KS, Takeda K, Yu ZY, Ferrans VJ, Finkel T. A role for reactive oxygen species in endothelial cell Anoikis. Circ Res. 1999;85(4):304–10.
14. Lu J, Tan M, Cai Q. The Warburg effect in tumor progression: mitochondrial oxidative metabolism as an anti-metastasis mechanism. Cancer Lett. 2015;356(2 Pt A):156–64.
15. Jiang X, Stockwell BR, Conrad M. Ferroptosis: mechanisms, biology and role in disease. Nat Rev Mol Cell Biol. 2021;22(4):266–82.
16. Dixon SJ, Lemberg KM, Lamprecht MR, Skouta R, Zaitsev EM, Gleason CE, Patel DN, Bauer AJ, Cantley AM, Yang WS, et al. Ferroptosis: an iron-dependent form of nonapoptotic cell death. Cell. 2012;149(5):1060–72.
17. Stockwell BR, Jiang X, Gu W. Emerging mechanisms and disease relevance of ferroptosis. Trends Cell Biol. 2020;30(6):478–90.
18. Zheng J, Conrad M. The metabolic underpinnings of ferroptosis. Cell Metab. 2020;32(6):920–37.
19. Yang WS, SriRamaratnam R, Welsch ME, Shimada K, Skouta R, Viswanathan VS, Cheah JH, Clemons PA, Shamji AF, Clish CB, et al. Regulation of ferroptotic cancer cell death by GPX4. Cell. 2014;156(1–2):317–31.
20. Friedmann AJ, Schneider M, Proneth B, Tyurina YY, Tyurin VA, Hammond VJ, Herbach N, Aichler M, Walch A, Eggenhofer E, et al. Inactivation of the ferroptosis regulator Gpx4 triggers acute renal failure in mice. Nat Cell Biol. 2014;16(12):1180–91.
21. Doll S, Freitas FP, Shah R, Aldrovandi M, Da SM, Ingold I, Goya GA, Xavier DST, Panzilius E, Scheel CH, et al. FSP1 is a glutathione-independent ferroptosis suppressor. Nature. 2019;575(7784):693–8.
22. Bersuker K, Hendricks JM, Li Z, Magtanong L, Ford B, Tang PH, Roberts MA, Tong B, Maimone TJ, Zoncu R, et al. The CoQ oxidoreductase FSP1 acts parallel to GPX4 to inhibit ferroptosis. Nature. 2019;575(7784):688–92.
23. Kraft V, Bezjian CT, Pfeiffer S, Ringelstetter L, Muller C, Zandkarimi F, Merl-Pham J, Bao X, Anastasov N, Kossl J, et al. GTP cyclohydrolase 1/tetrahydrobiopterin counteract ferroptosis through lipid remodeling. ACS Cent Sci. 2020;6(1):41–53.
24. Soula M, Weber RA, Zilka O, Alwaseem H, La K, Yen F, Molina H, Garcia-Bermudez J, Pratt DA, Birsoy K. Metabolic determinants of cancer cell sensitivity to canonical ferroptosis inducers. Nat Chem Biol. 2020;16(12):1351–60.
25. Bai Y, Meng L, Han L, Jia Y, Zhao Y, Gao H, Kang R, Wang X, Tang D, Dai E. Lipid storage and lipophagy regulates ferroptosis. Biochem Biophys Res Commun. 2019;508(4):997–1003.
26. Sattari FF, Jalilzadeh N, Mehdizadeh A, Sajjadian F, Velaei K. Understanding and targeting Anoikis in metastasis for cancer therapies. Cell Biol Int. 2023;47(4):683–98.

27. Buchheit CL, Weigel KJ, Schafer ZT. Cancer cell survival during detachment from the ECM: multiple barriers to tumour progression. Nat Rev Cancer. 2014;14(9):632–41.
28. Du S, Yang Z, Lu X, Yousuf S, Zhao M, Li W, Miao J, Wang X, Yu H, Zhu X, et al. Anoikis resistant gastric cancer cells promote angiogenesis and peritoneal metastasis through C/EBPbeta-mediated PDGFB autocrine and paracrine signaling. Oncogene. 2021;40(38):5764–79.
29. Bailey AP, Koster G, Guillermier C, Hirst EM, MacRae JI, Lechene CP, Postle AD, Gould AP. Antioxidant role for lipid droplets in a stem cell niche of Drosophila. Cell. 2015;163(2):340–53.
30. Schulze RJ, Krueger EW, Weller SG, Johnson KM, Casey CA, Schott MB, McNiven MA. Direct lysosome-based autophagy of lipid droplets in hepatocytes. Proc Natl Acad Sci U S A. 2020;117(51):32443–52.
31. Butler LM, Perone Y, Dehairs J, Lupien LE, de Laat V, Talebi A, Loda M, Kinlaw WB, Swinnen JV. Lipids and cancer: emerging roles in pathogenesis, diagnosis and therapeutic intervention. Adv Drug Deliv Rev. 2020;159:245–93.
32. Xia Z, Zhou X, Li J, Li L, Ma Y, Wu Y, Huang Z, Li X, Xu P, Xue M. Multiple-Omics techniques reveal the role of glycerophospholipid metabolic pathway in the response of Saccharomyces cerevisiae against hypoxic stress. Front Microbiol. 2019;10:1398.
33. Rusu P, Shao C, Neuerburg A, Acikgoz AA, Wu Y, Zou P, Phapale P, Shankar TS, Doring K, Dettling S, et al. GPD1 specifically marks dormant glioma stem cells with a distinct metabolic profile. Cell Stem Cell. 2019;25(2):241–e2578.
34. Yao CH, Park JS, Kurmi K, Hu SH, Notarangelo G, Crowley J, Jacobson H, Hui S, Sharpe AH, Haigis MC. Uncoupled glycerol-3-phosphate shuttle in kidney cancer reveals that cytosolic GPD is essential to support lipid synthesis. Mol Cell. 2023;83(8):1340–e13497.
35. Turyn J, Schlichtholz B, Dettlaff-Pokora A, Presler M, Goyke E, Matuszewski M, Kmiec Z, Krajka K, Swierczynski J. Increased activity of glycerol 3-phosphate dehydrogenase and other lipogenic enzymes in human bladder cancer. Horm Metab Res. 2003;35(10):565–9.
36. Ye Y, Chen A, Li L, Liang Q, Wang S, Dong Q, Fu M, Lan Z, Li Y, Liu X, et al. Repression of the antiporter SLC7A11/glutathione/glutathione peroxidase 4 axis drives ferroptosis of vascular smooth muscle cells to facilitate vascular calcification. Kidney Int. 2022;102(6):1259–75.
37. Bebber CM, Muller F, Prieto CL, Weber J, von Karstedt S. Ferroptosis Cancer Cell Biology Cancers (Basel). 2020;12(1):164.
38. Li W, Liang L, Liu S, Yi H, Zhou Y. FSP1: a key regulator of ferroptosis. Trends Mol Med. 2023;29(9):753–64.
39. Nakamura T, Hipp C, Santos DMA, Borggrafe J, Aldrovandi M, Henkelmann B, Wanninger J, Mishima E, Lytton E, Emler D, et al. Phase separation of FSP1 promotes ferroptosis. Nature. 2023;619(7969):371–7.
40. Gao G, Xie Z, Li EW, Yuan Y, Fu Y, Wang P, Zhang X, Qiao Y, Xu J, Holscher C, et al. Dehydroabietic acid improves nonalcoholic fatty liver disease through activating the Keap1/Nrf2-ARE signaling pathway to reduce ferroptosis. J Nat Med. 2021;75(3):540–52.

Publisher's note

Springer Nature remains neutral with regard to jurisdictional claims in published maps and institutional affiliations.